Supercritical CO$_2$ Power Cycles: Design Considerations for

Concentrating Solar Power

Ty Neises	**Craig Turchi**
Research Engineer	Sr. Research Engineer
National Renewable Energy Laboratory	National Renewable Energy Laboratory
Golden, Colorado, USA	Golden, Colorado, USA
ty.neises@nrel.gov	craig.turchi@nrel.gov

ABSTRACT

A comparison of three supercritical CO$_2$ Brayton cycles: the simple cycle, recompression cycle and partial-cooling cycle indicates the partial-cooling cycle is favored for use in concentrating solar power (CSP) systems. Although it displays slightly lower cycle efficiency versus the recompression cycle, the partial-cooling cycle is estimated to have lower total recuperator size, as well as a lower maximum s-CO$_2$ temperature in the high-temperature recuperator. Both of these effects reduce recuperator cost. Furthermore, the partial-cooling cycle provides a larger temperature differential across the turbine, which translates into a smaller, more cost-effective thermal energy storage system. The temperature drop across the turbine (and by extension, across a thermal storage system) for the partial-cooling cycle is estimated to be 23% to 35% larger compared to the recompression cycle of equal recuperator conductance between 5 and 15 MW/K. This reduces the size and cost of the thermal storage system. Simulations by NREL and Abengoa Solar indicate the partial-cooling cycle results in a lower LCOE compared with the recompression cycle, despite the former's slightly lower cycle efficiency. Advantages of the recompression cycle include higher thermal efficiency and potential for a smaller precooler. The overall impact favors the use of a partial-cooling cycle for CSP compared to the more commonly analyzed recompression cycle.

BACKGROUND and OBJECTIVE

Closed-loop supercritical CO$_2$ (s-CO$_2$) Brayton cycles are being investigated for multiple applications including fossil, nuclear, and concentrating solar power (CSP) generation plants. These cycles are projected to achieve higher cycle efficiency compared to steam Rankine cycles at temperatures achievable or proposed for these applications. Additionally, these cycles are projected to have a smaller mass and complexity versus the Rankine power block. A feature of s-CO$_2$ cycles is that multiple configurations of turbomachinery and heat exchangers can be constructed to yield similar overall efficiency but different temperature and/or pressure characteristics relevant to the application of interest. This attribute suggests that the optimum power cycle configuration may be a function of the specific heat source.

Three factors distinguish the CSP power block application: 1) superior performance in hot, arid climates with dry cooling, 2) the ability to economically integrate thermal energy storage, and 3) frequent cycling. Due to its single-phase operation, s-CO$_2$ systems are a good match for efficient heat exchange with sensible heat storage such as the molten salts used in commercial CSP plants. The mass and cost of sensible heat storage required per MWh is proportional to the temperature difference between the hot and cold storage conditions; thus, power cycles that enable larger temperature differentials across the storage unit are desired. This paper examines the thermal efficiency and cross-turbine temperature differences of different cycle configurations with the goal of optimizing a cycle for a CSP plant with thermal energy storage.

APPROACH

The following analysis evaluates the simple, recompression, and partial cooling models shown in Figure 1. The cycle components included in the design point models are compressors, turbines, and heat exchangers (recuperators and precoolers). The turbomachinery components are modeled with a simple isentropic efficiency model.
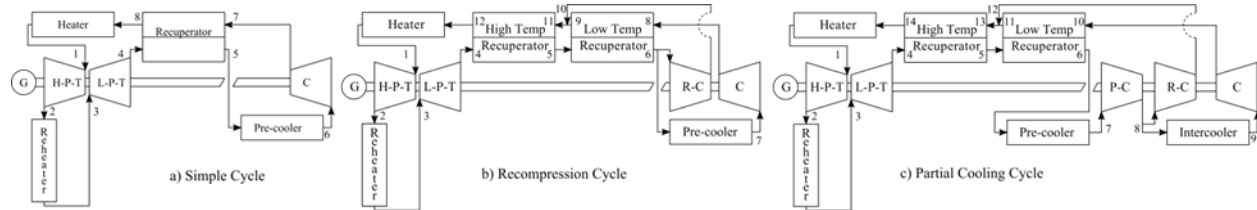

Figure 1. Closed-loop s-CO$_2$ Brayton cycles studied in this paper.

The counter-flow recuperator modeling approach depends on whether an effectiveness or conductance is specified to characterize the recuperator. Both models discretize the heat exchanger to account for changing physical properties and solve for the conditions that result in the specified effectiveness or conductance [10]. The effectiveness model may also enforce a minimum temperature difference in the recuperator that is designed to constrain the performance of the recuperator by imposing "realistic" physical bounds (although quantifying the exact impact of this constraint is difficult without using the more detailed conductance model). Validation of the effectiveness model is shown in the previous work [10]. The conductance model uses the standard counter-flow effectiveness-NTU relationship at each discretization to calculate the total heat exchanger conductance. Note that the conductance model is sensitive to the power rating of the cycle while the effectiveness model is not. The precooler was not studied in this analysis. An air-cooled finned-tube precooler model was developed as a thesis project by Gavic [7].

These components were coded as subprograms or procedures in Engineering Equation Solver (EES) [8]. The cycle model solves by calling these subprograms/procedures as necessary and applying the following assumptions and constraints:

- The turbine inlet temperature is set as a constant value. This value is not optimized as it is known that increasing it will increase cycle efficiency. The model assumes that a primary heat exchanger exists that can meet the required thermal input and turbine inlet temperature.

- The compressor inlet temperature is set as a constant value. In a more detailed design study, this value may be optimized along with precooler size and cooling fan parasitic.

- In the recompression and partial-cooling cycles, the model is constrained such that the compressor outlet temperature of the flow that bypasses the low temperature recuperator is set equal to the high pressure outlet temperature of the recuperator (i.e., the temperatures at points 9, 10, and 11 are equal in Figure 1a, and the temperatures 11, 12, and 13 are equal in Figure 1b). This approach is consistent with the literature.

- Pressure drops in the heat exchangers are neglected.

- One stage of reheat is modeled for each configuration. The intermediate pressure is set as the average of the high and low side pressures [5]. This analysis does not address if the cycle-efficiency benefit of single-stage reheat will justify the additional system complexity; however, the impact is applied across all cycles in this analysis so cycle-to-cycle comparisons should remain valid.

- Heat exchanger performance is defined by specifying a performance metric, which depends on the heat exchanger model used. In the recompression and partial-cooling cycles using the effectiveness approach, the high temperature recuperator and overall hot side effectiveness are specified, which matches Dostal's approach [9]. When the conductance model is applied, the combined recuperator conductance and the fraction of conductance allotted to the high temperature recuperator are specified. It is clear that increasing the combined conductance will

improve cycle efficiency (at least for the current case ignoring pressure drops). However, it is not intuitive how the combined recuperator conductance should be allocated between the high and low temperature recuperators for the recompression and partial cooling cycles. Therefore, the fraction allocated to the high temperature recuperator is optimized for each design case.

- The maximum system pressure (P_{high}) is set to a constant value. The pressure ratio, which defines the lower pressure, is optimized for each design case.

- The partial cooling cycle requires an intermediate compressor pressure. This value is defined by the ratio of pressure ratios (rpr), and is also optimized for each design case:

$$rpr = \frac{(P_{high}/P_{intermediate}) - 1}{(P_{high}/P_{low}) - 1} \qquad (1)$$

- All optimization was completed using the "Variable Metric" method built into EES.

Design values

Table 1 shows the values of the design parameters used in this study, along with brief comments explaining their selection. The values in this table fully constrain the model and allow for the modeling results presented in the next section to be reproduced.

Table 1: Design and optimized parameters for cycle case studies

Design Parameters	Value	Comments
Turbine efficiency	93%	Projection of mature, commercial size axial flow turbine efficiency
Compressor efficiency	89%	Projection of mature, commercial size radial compressor
Heat exchanger effectiveness	97%	5°C minimum temperature difference, neglect pressure drops
Heat exchanger conductance (UA)	Varied MW/K	Neglect pressure drops
Turbine inlet temperature	650°C	SunShot target for CSP power tower outlet temperatures
Compressor inlet temperature	50°C	Possible under dry cooling with 10°C ITD, 40°C ambient temperature
Maximum pressure	25 MPa	Upper limit given available and economic piping
Reheat	yes	One stage of reheat at average of high and low side pressures
Net power output	35 MW	Estimate of power cycle requirements for a 100 MW-thermal SunShot-target power tower with thermal energy storage

Optimized Parameters	Relevant Cycles
Pressure ratio (PR)	All
f_{HTR}	Recompression, Partial Cooling (not applicable for effectiveness approach)
Ratio of pressure ratios (rpr)	Partial Cooling

RESULTS

First, the effectiveness/minimum-temperature approach is optimized for each configuration using the design conditions in Table 1, and the required recuperator conductance is calculated. The results in Table 2 show that for the selected design conditions, the recompression cycle conductance is almost twice as large as the partial-cooling cycle conductance, while achieving an only slightly improved thermal efficiency. The simple cycle has the lowest conductance, but suffers a 5% efficiency penalty.

Table 2: Optimized modeling results using effectiveness model and design effectiveness to model recuperator

Cycle	PR	rpr	*Gross Efficiency	Split Fraction	UA LTR	UA HTR	UA Combined
	-	-	%	-	MW/K	MW/K	MW/K
Simple	3.4	-	44.60	-	-	3.04	3.04
Recompression	2.5	-	49.66	0.71	3.21	5.33	8.54
Partial Cooling	4.55	0.369	49.53	0.59	1.73	2.60	4.33
*Note that the reported thermal efficiency does not include precooler fan parasitics.							

Because of the large difference in calculated conductance when the recuperator effectiveness/minimum-temperature model is used, it is difficult to compare the cycle performance on an equivalent basis. To better understand the relationship between cycle performance and conductance, each cycle configuration was solved using the conductance model for the recuperator over a range of values. Figure 2 shows that when the cycles are compared with equal conductance values, the partial cooling cycle asymptotes towards its highest efficiency at much lower conductance values than the recompression cycle. Additionally, this analysis shows the overlap at low conductance values between the simple and recompression cycles that has been observed by others [1,6].
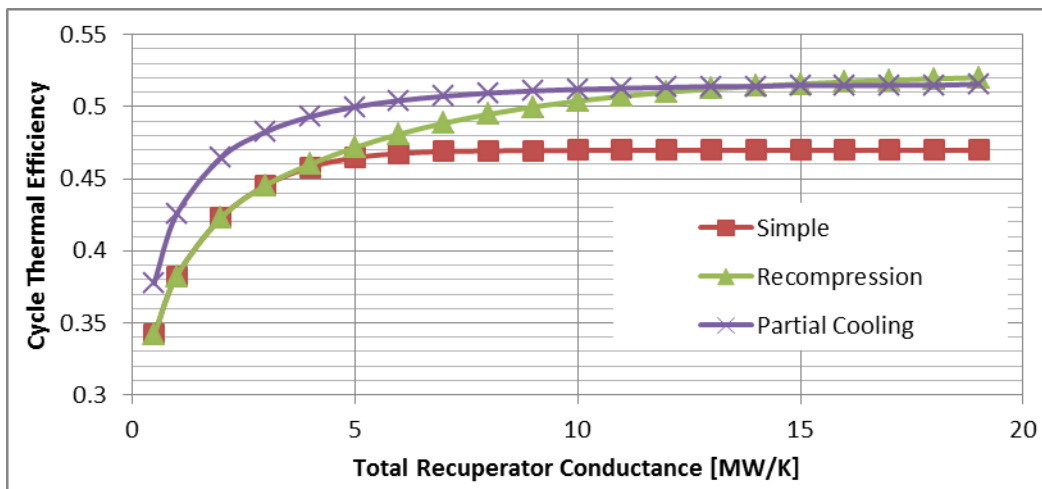

Figure 2. Optimized cycle thermal efficiency versus total recuperator conductance

If it can be assumed that cycle cost is largely driven by the required recuperator conductance, then the partial-cooling cycle appears advantageous at these design conditions up to about 15 MW/K of conductance. Table 3 shows additional relevant cycle metrics at three different conductance levels. It is also notable that the high temperature recuperator in the partial-cooling cycle experiences a maximum temperature around 50°C lower than the recompression cycle, which may help reduce its relative cost. The recompression cycle rejects all of its heat at higher pressures, which provides a more favorable temperature profile for heat rejection [4], and may result in a smaller precooler.

Table 3: Optimized modeling results using conductance model to model recuperator at various levels of conductance

Cycle	Recup UA	f_{HTR}	P_{low}	P_{inter}	*Gross Efficiency	Split Fraction	ΔT PHX
	MW/K	-	MPa	MPa	%	-	°C
Recompression	5	0.497	8.56	-	47.17	0.87	138.0
Partial Cooling	5	0.564	5.58	10.61	49.99	0.60	180.5
Recompression	10	0.568	10.0	-	50.39	0.73	114.2
Partial Cooling	10	0.454	5.96	10.90	51.21	0.59	170.5
Recompression	15	0.535	10.05	-	51.59	0.70	109.5
Partial Cooling	15	0.375	6.06	10.95	51.49	0.60	168.4
*Note that the reported thermal efficiency does not include fan parasitics.							

Figure 3 shows a comparison of the recompression and partial-cooling cycles on a temperature-entropy diagram for the 15 MW/K conductance case. This plot emphasizes some of the important tabular data and helps explain how each cycle derives its efficiency. As listed in Table 3 and shown in this figure, the partial-cooling cycle optimizes at a higher pressure ratio. This feature is afforded to the cycle by the intercooler (intermediate pressure precooler). The higher pressure ratio causes the outlet temperature of the low pressure turbine to be lower than it is in the recompression cycle. In turn, the average heat input temperature is lower for the partial-cooling cycle, which all else equal results in lower cycle efficiency. One mitigating effect, however, is that the intercooling stage allows for a lower pressure difference across the main compressor. Consequently, the compressor outlet temperature is lower for the partial-cooling cycle, thereby decreasing the high pressure, low temperature recuperator outlet temperature and allowing the cycle to reject heat at a lower average temperature. Finally, the higher pressure ratio results in a lower required mass flow rate to generate a given amount of power. Therefore, recuperators in the partial-cooling cycle will have a lower duty, and it follows that for a fixed recuperator conductance the cycle with the lower duty will likely experience greater effectiveness in the recuperators.
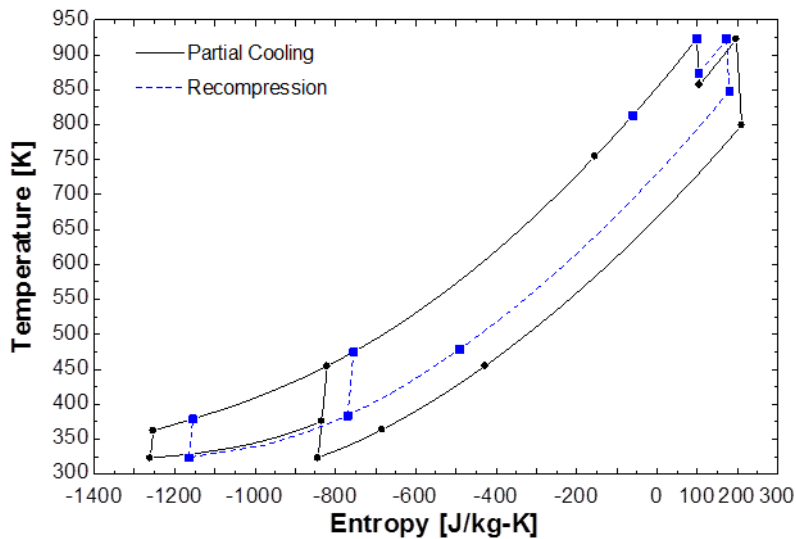

Figure 3. Temperature-entropy diagram of optimized cycles with 15 MW/K recuperator conductance

Model Limitations

Figure 2 suggests that the partial-cooling cycle offers an efficiency advantage over the recompression cycle at most values of recuperator conductance. The purpose of this study was to compare the selected cycles on an equivalent basis using recuperator conductance model that can be used as a proxy for the total heat exchanger size used, and therefore, the cost. While these models improve upon the effectiveness model used in previous analyses, they do contain assumptions that likely impact the results:

- The conductance model (along with the entire cycle model) does not consider pressure drops. Therefore, the density of the fluid has no impact on heat exchanger size. For example, a lower density fluid may require a trade-off between more cross-sectional flow area and a higher pressure drop. The low-side stream in the partial-cooling cycle will have a lower density than the low-side stream in the recompression cycle.
- The conductance model does not consider the effect of absolute pressures and pressure differentials on the material thicknesses (and therefore conductance) of the heat exchangers. The partial-cooling cycle has a larger pressure ratio than the recompression cycle; however, it has a lower absolute pressure.
- The conductance model does not calculate the convective heat transfer coefficients of the fluid, and therefore does not assess possible differences in conductance between cycles due to varying fluid properties.

The precooler mass size and performance is not considered in this study. In reality, the cycle model would be optimized concurrently with a precooler model. For example, the fan power might be increased to limit the total precooler mass, or the compressor inlet temperature or pressure ratio may be adjusted to achieve more favorable cooling conditions at the expense of cycle efficiency.

Cycle integration with CSP systems

Recent work has highlighted the economic benefit of CSP plants with thermal storage [2,3]. Sensible heat storage systems have been commercialized at temperatures around 560°C and are being researched for higher temperatures to meet DOE SunShot objectives. The temperature difference between the inlet and outlet of the primary heat exchanger has a direct impact on the cost of a sensible thermal energy storage system, given that the mass of required storage media for a fixed amount of thermal storage capacity is inversely proportional to $C_p\Delta T$. Table 3 shows that this temperature difference in the partial-cooling cycle is between 23% and 35% larger than in the recompression cycle, depending on the recuperator conductance. This may result in cost savings for sensible heat thermal storage integrated with a partial-cooling cycle at SunShot conditions [4]. Furthermore, the partial-cooling cycle maintains its larger temperature difference across the primary heat exchanger at current power tower conditions (~565°C), although the impact of lower temperatures on the cycle efficiency relative to the recompression cycle has not been analyzed.

Finally, the partial-cooling cycle grants greater potential to lower the high pressure in the cycle. Figure 4 shows that at an upper pressure of 20 MPa the partial-cooling cycle nearly matches the performance of the design cases at 25 MPa, while the recompression cycle at 20 MPa suffers a proportionally larger efficiency penalty until large recuperator conductance values are included. The lower pressure design may be particularly suited for direct receiver applications (i.e., where s-CO$_2$ is heated directly in the solar receiver) as the combination of high pressure and high temperature causes the required tube thickness to significantly increase. By decreasing the pressure, the design gains flexibility to decrease thickness, and possibly increase the allowable incident flux or receiver fatigue life. It should be noted that the partial-cooling cycle at 20 MPa operates at a lower pressure ratio, which decreases the temperature difference over the primary heat exchanger. The model shows that at 10 MW/K the 20 MPa model has a temperature difference of 161.5°C, while the 25 MPa model has a difference of 170.5°C and the recompression cycle at 20 MPa has a difference of 114.2°C.
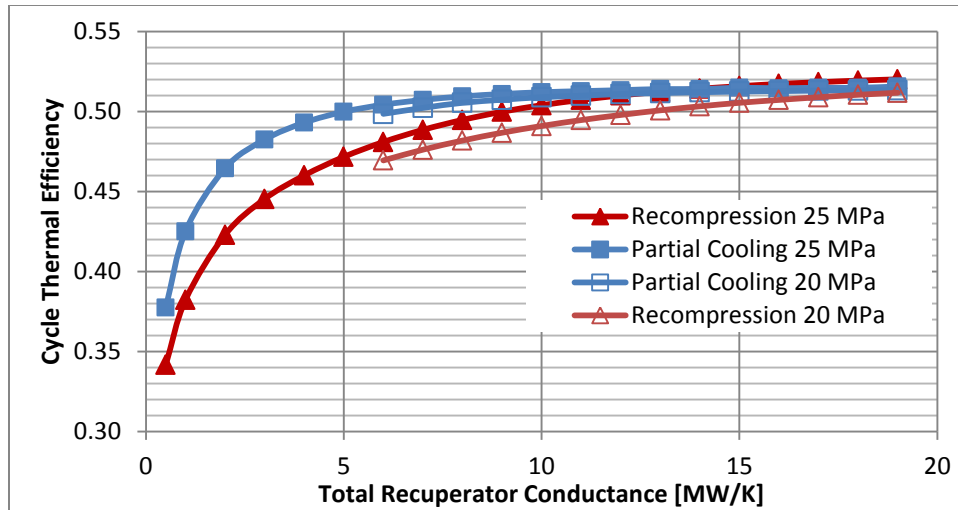
Figure 4. Analysis of optimized cycle thermal efficiency vs. recuperator conductance at 20 and 25 MPa upper pressures

Analysis by Abengoa Solar concurred that the partial-cooling cycle was preferred over the recompression cycle despite a lower cycle efficiency [11]. In annual simulations, the partial-cooling cycle resulted in a lower plant levelized cost of energy (LCOE) due to lower recuperator cost and a larger temperature differential across storage compared to the recompression cycle. The analysis found the LCOE of current molten-salt power tower technology can be lowered by replacing the steam Rankine power block with an s-CO_2 cycle. An 8% LCOE reduction was projected versus the current state of the art, assuming a partial-cooling s-CO_2 cycle mated with a solar-salt power tower with a receiver outlet temperature of 600°C. A 13.5% reduction was possible using pure $NaNO_3$ salt and assumed reductions in recuperator costs based on discussion with teams developing new heat exchanger designs for s-CO_2 systems.

CONCLUSIONS

A comparison of the three cycle options indicates the following advantages of a partial-cooling cycle for a CSP application:

- When compared with equal conductance values, the partial-cooling cycle asymptotes towards its peak efficiency at much lower conductance values than the recompression cycle. This offers the advantage of much smaller recuperators with little penalty in cycle efficiency.

- The temperature drop across the turbine (and by extension, across a thermal storage system) for the partial-cooling cycle is 23% to 35% larger compared to the recompression cycle of equal recuperator conductance between 5 and 15 MW/K. This reduces the size and cost of the thermal storage system.

- The maximum temperature in the high-temperature recuperator is approximately 50K lower in the partial-cooling cycle, which may help reduce its material cost.

- Annual simulations by NREL and Abengoa Solar indicate the partial-cooling cycle results in a lower LCOE compared with the recompression cycle, despite the former's slightly lower cycle efficiency.

Advantages of the recompression cycle include one less compressor and higher potential thermal efficiency. The overall impact favors the use of a partial-cooling cycle for CSP compared to the more commonly analyzed recompression cycle. The recompression cycle collapses to the simple cycle at low values of total recuperator UA.

NOMENCLATURE

C_p Thermal storage fluid specific heat capacity, [kJ/kg-K]

CSP   Concentrating Solar Power

f_{HTR} Fraction of total conductance allocated to the high temperature recuperator

LTR   Low temperature recuperator

HTR   High temperature recuperator

P   Pressure, [MPa]

PHX   Primary heat exchanger

PR   Pressure ratio across the power turbine(s)

UA   Heat exchanger conductance, [MW/K]

REFERENCES

[1] Bryant, J.C., H. Saari, and K. Zanganeh, "An Analysis and Comparison of the Simple and Recompression Supercritical CO_2 Cycles," Supercritical CO_2 Power Cycle Symposium, Boulder, Colorado, 2011.

[2] Denholm, P., Y. Wan, M. Hummon, and M. Mehos, "An Analysis of Concentrating Solar Power with Thermal Energy Storage in a California 33 % Renewable Scenario An Analysis of Concentrating Solar Power with Thermal Energy Storage in a California 33 % Renewable Scenario," 2013.

[3] Denholm, P., and M. Mehos, "Enabling Greater Penetration of Solar Power via the Use of CSP with Thermal Energy Storage," NREL, Golden, CO, 2011.

[4] DOE SunShot goals at http://energy.gov/eere/sunshot/concentrating-solar-power

[5] Dostal, V., M. J. Driscoll, and P. Hejzlar, "Advanced Nuclear Power Technology Program A Supercritical Carbon Dioxide Cycle for Next Generation Nuclear Reactors," MIT, 2004.

[6] Dyreby, J.J., S.A. Klein, G.F. Nellis, and D.T. Reindl, "Development of Advanced Models for Supercritical Carbon Dioxide Power Cycles for Use in Concentrating Solar Power Systems - Subcontract No. AXL-0-40301-1 to National Renewable Energy Laboratory," 2012.

[7] Gavic, D.J., "Investigation of Water, Air, and Hybrid Cooling for Supercritical Carbon Dioxide Brayton Cycles," University of Wisconsin-Madison, 2012.

[8] Klein, S.A., EES – Engineering Equation Solver, F-Chart Software. http://www.fchart.com.," p. 2010, 2010.

[9] Kulhánek, M., and V. Dostal, "Thermodynamic Analysis and Comparison of Supercritical Carbon Dioxide Cycles," 2011 Supercritical CO_2 Power Cycle Symposium, Boulder, Colorado, 2011.

[10] Turchi, C.S., Z. Ma, T. Neises, and M. Wagner, "Thermodynamic Study of Advanced Supercritical Carbon Dioxide Power Cycles for High Performance Concentrating Solar Power Systems - Preprint," in Proceedings of ASME 2012 6th International Conference on Energy Sustainability & 9th Fuel Cell Science, Engineering and Technology Conference, 2012.

[11] Turchi, C.S., "10 MW Supercritical CO2 Turbine Test," Final Report under DE-EE0001589, National Renewable Energy Laboratory, January 27, 2014, available online at www.OSTI.gov.

ACKNOWLEDGEMENTS